Infimal Convolution Type Coupling of First and Second Order Differences on Manifold-valued Images

Ronny Bergmann, Jan Henrik Fitschen,
Johannes Persch, Gabriele Steidl
Technische Universität Kaiserslautern

6th International Conference on Scale Space and Variational Methods in Computer Vision

Kolding, Denmark, June 6, 2017

Contents

1. Manifold-valued image processing
2. Total variation and Infimal convolution
3. An extrinsic model
4. An intrinsic model
5. Examples

Manifold-valued image processing

New data aquisition modalities $\Rightarrow$ non-Euclidean range of data

- Interferrometric synthetic aperture radar (InSAR)
- Surface normals
- Diffusion tensors in magnetic resonance imaging (DT-MRI)
- Electron backscattered diffraction (EBSD)
- Directional data: wind, flow, GPS,...

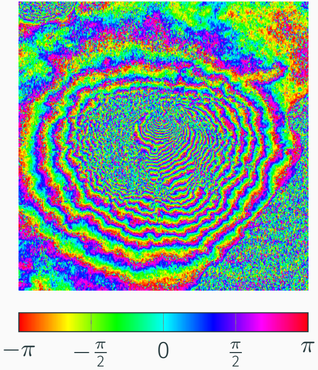

InSAR data of Mt. Vesuvius
[Rocca, Prati, Guarnieri 1997]

$\mathbb{S}^1$

Manifold-valued image processing

New data aquisition modalities $\Rightarrow$ non-Euclidean range of data

- Interferrometric synthetic aperture radar (InSAR)
- Surface normals
- Diffusion tensors in magnetic resonance imaging (DT-MRI)
- Electron backscattered diffraction (EBSD)
- Directional data: wind, flow, GPS,...

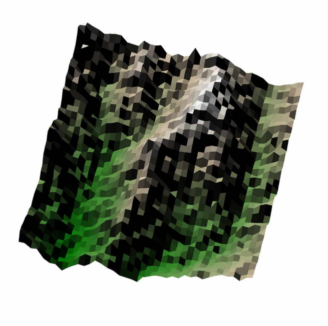

National elevation dataset
[Gesch, Evans, Mauck, 2009; MFOPT/Lellmann]

$\mathbb{S}^2$

Manifold-valued image processing

New data aquisition modalities $\Rightarrow$ non-Euclidean range of data

- Interferrometric synthetic aperture radar (InSAR)
- Surface normals
- Diffusion tensors in magnetic resonance imaging (DT-MRI)
- Electron backscattered diffraction (EBSD)
- Directional data: wind, flow, GPS,...

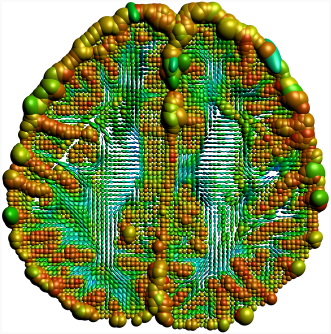

Slice # 28 from the Camino data set
http://cmic.cs.ucl.ac.uk/camino

3×3, sym. pos. def. matrices

Manifold-valued image processing

New data aquisition modalities $\Rightarrow$ non-Euclidean range of data

- Interferrometric synthetic aperture radar (InSAR)
- Surface normals
- Diffusion tensors in magnetic resonance imaging (DT-MRI)
- Electron backscattered diffraction (EBSD)
- Directional data: wind, flow, GPS,...

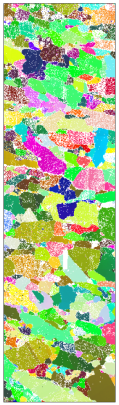

EBSD example from the MTEX toolbox
[Bachmann, Hielscher, since 2005]

$\mathrm{SO}(3)$ (mod. symmetry)

Manifold-valued image processing

New data aquisition modalities ⇒ non-Euclidean range of data

- Interferrometric synthetic aperture radar (InSAR)
- Surface normals
- Diffusion tensors in magnetic resonance imaging (DT-MRI)
- Electron backscattered diffraction (EBSD)
- Directional data: wind, flow, GPS,...

Similarities

- Range of the pixel is a Riemannian manifold
- Tasks of "classical" image processing

Notations on a Riemannian manifold $\mathcal{M}$

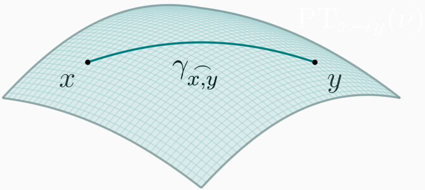

"A d-dimensional manifold can be informally defined as a set $\mathcal{M}$ covered with a 'suitable' collection of charts, that identify subsets of $\mathcal{M}$ with open subsets of $\mathbb{R}^d$."

[Absil, Mahony, Sepulchre, 2008]

Notations on a Riemannian manifold $\mathcal{M}$

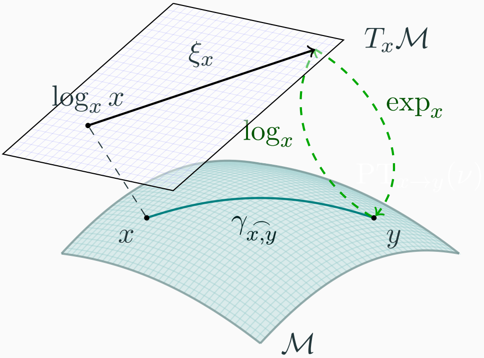

geodesic $\gamma_{\widehat{x,y}}$ shortest path (on $\mathcal{M}$) connecting $x, y \in \mathcal{M}$.
tangential plane $\mathrm{T}_x\mathcal{M}$ at x, $\mathrm{T}\mathcal{M} \coloneqq \cup_{x\in\mathcal{M}}\mathrm{T}_x\mathcal{M}$
logarithmic map $\log_x y = \dot{\gamma}_{\widehat{x,y}}(0)$, "velocity towards y"
exponential map $\exp_x \xi_x = \gamma(1)$, where $\gamma(0) = x$, $\dot{\gamma}(0) = \xi_x$

Real- and vector-valued first and second order TV

- $\mathcal{G} = \{1,\ldots,N_1\} \times \{1,\ldots,N_2\}$ the pixel grid, $\mathcal{V} \subset \mathcal{G}$
- $\mathcal{N}_p = \{p + (0,1), p + (1,0)\} \cap \mathcal{G}$ the neighbors of $p \in \mathcal{G}$

Given data $f\colon \mathcal{V} \to \mathbb{R}^n$ reconstruct original data u_0 by minimizing the Variational Model

$$\mathcal{E}(u) \coloneqq \underbrace{\mathcal{D}(u;f)}_{\text{data term}} + \underbrace{\alpha\,\mathcal{R}(u)}_{\text{regularization term}}, \qquad \alpha > 0.$$

Real- and vector-valued first and second order TV

- $\mathcal{G} = \{1, \ldots, N_1\} \times \{1, \ldots, N_2\}$ the pixel grid, $\mathcal{V} \subset \mathcal{G}$
- $\mathcal{N}_p = \{p + (0,1), p + (1,0)\} \cap \mathcal{G}$ the neighbors of $p \in \mathcal{G}$

Given data $f\colon \mathcal{V} \to \mathbb{R}^n$ reconstruct original data u_0 by minimizing the Variational Model

$$\mathcal{E}(u) := \underbrace{\mathcal{D}(u; f)}_{\text{data term}} + \underbrace{\alpha\, \mathcal{R}(u)}_{\text{regularization term}}, \qquad \alpha > 0.$$

- total variation $$\operatorname{TV}(u) := \sum_{p \in \mathcal{G}} \sqrt{\sum_{q \in \mathcal{N}_p} (u_q - u_p)^2}$$

[Rudin, Osher, Fatemi, 1992]

Real- and vector-valued first and second order TV

- $\mathcal{G} = \{1,\ldots,N_1\} \times \{1,\ldots,N_2\}$ the pixel grid, $\mathcal{V} \subset \mathcal{G}$
- $\mathcal{N}_p = \{p+(0,1), p+(1,0)\} \cap \mathcal{G}$ the neighbors of $p \in \mathcal{G}$

Given data $f\colon \mathcal{V} \to \mathbb{R}^n$ reconstruct original data u_0 by minimizing the Variational Model

$$\mathcal{E}(u) \coloneqq \underbrace{\mathcal{D}(u;f)}_{\text{data term}} + \underbrace{\alpha\,\mathcal{R}(u)}_{\text{regularization term}}, \qquad \alpha > 0.$$

- total variation $\quad \operatorname{TV}(u) \coloneqq \sum_{p\in\mathcal{G}} \sqrt{\sum_{q\in\mathcal{N}_p} (u_q - u_p)^2}$
- second order TV $\operatorname{TV}_2(u) \coloneqq \sum_{p\in\mathcal{G}} \sqrt{d_{2,\mathrm{h}}^2(u_p) + d_{2,\mathrm{v}}^2(u_p)}$

[Chambolle, Lions, 1997; Bredies, Kunisch, Pock, 2010; Setzer, Steidl, 2008; Papafitsoros, Schönlieb, 2014]

Real- and vector-valued first and second order TV

- $\mathcal{G} = \{1, \dots, N_1\} \times \{1, \dots, N_2\}$ the pixel grid, $\mathcal{V} \subset \mathcal{G}$
- $\mathcal{N}_p = \{p + (0,1), p + (1,0)\} \cap \mathcal{G}$ the neighbors of $p \in \mathcal{G}$

Given data $f \colon \mathcal{V} \to \mathbb{R}^n$ reconstruct original data u_0 by minimizing the Variational Model

$$\mathcal{E}(u) := \underbrace{\mathcal{D}(u; f)}_{\text{data term}} + \underbrace{\alpha\, \mathcal{R}(u)}_{\text{regularization term}}, \qquad \alpha > 0.$$

- total variation $\quad \mathrm{TV}(u) := \sum_{p \in \mathcal{G}} \sqrt{\sum_{q \in \mathcal{N}_p} (u_q - u_p)^2}$
- second order TV $\mathrm{TV}_2(u) := \sum_{p \in \mathcal{G}} \sqrt{d_{2,\mathrm{h}}^2(u_p) + d_{2,\mathrm{v}}^2(u_p)}$
- $d_{2,\mathrm{h}}(u_p) := \begin{cases} \|u_{p-(1,0)} - 2u_p + u_{p+(1,0)}\|_2, & 1 < p_1 < N_1, \\ 0, & \text{else.} \end{cases}$

Infimal convolution

For $f\colon \mathcal{G} \to \mathbb{R}^n$, $\alpha, \beta > 0$ minimize

Additive model:

$$E_{\mathrm{Add}}(u) := \frac{1}{2}\|f - u\|_2^2 + \alpha\left(\beta\,\mathrm{TV}(u) + (1-\beta)\,\mathrm{TV}_2(u)\right),$$

Infimal convolution model

$$E_{\mathrm{IC}}(u) := \frac{1}{2}\|f - u\|_2^2 + \alpha \min_{u=v+w}\left(\beta\,\mathrm{TV}(v) + (1-\beta)\,\mathrm{TV}_2(w)\right),$$

For manifold-valued data $f\colon \mathcal{G} \to \mathcal{M}$

- What's a second order difference?
- How to decompose $u\colon \mathcal{G} \to \mathcal{M}$ into two images v and w?

Extrinsic model of infimal convolution

$$E_{\mathrm{IC}}^{\mathrm{ext}}(u) \coloneqq \frac{1}{2}\|f-u\|_2^2+\alpha\bigl(\beta\,\mathrm{TV}\,\square(1-\beta)\,\mathrm{TV}_2\bigr)(u) \quad \text{s.t.} \quad u\in\mathcal{M}^N.$$

where

$$(F_1 \square F_2)(u) \coloneqq \inf_{u=v+w}\{F_1(v)+F_2(w)\} = \inf_{v}\{F_1(v)+F_2(u-v)\}.$$

- embed manifold in Euclidean space [Whitney, 1936; Nash, 1956]
- add manifold as constraint [Rosman et al., 2014]
- decomposition $u = v + w$ as before
- apply ADMM / Augmented Lagrangian on the Lie algebra

⊖ v and w have no interpretation on the manifold

First and second order differences on manifolds

- First order difference:

[Cremers, Strekalovskiy, 2011/2013; Lellmann et al. 2013; Weinmann et al., 2014]

$$d_{\mathcal{M}}(u_p, u_q), \quad u_p, u_q \in \mathcal{M}, q \in \mathcal{N}_p, p \in \mathcal{G}.$$

- Second order difference: [RB et al., 2014; RB, Weinmann, 2016; Bačák et al., 2016]

$$\mathrm{d}_2(x, y, z) \coloneqq \min_{c \in \mathcal{C}_{x,z}} \mathrm{d}_{\mathcal{M}}(c, y), \quad x, y, z \in \mathcal{M},$$

$\mathcal{C}_{x,z}$ mid points of geodesic(s) $\gamma_{\widehat{x,z}}$

$\frac{1}{2}\|x - 2y + z\|_2 = \|\frac{1}{2}(x+z) - y\|_2$

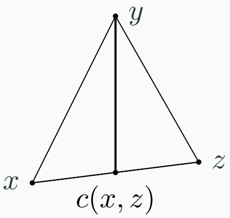

$\min_{c \in \mathcal{C}_{x,z}} d_{\mathcal{M}}(c, y)$

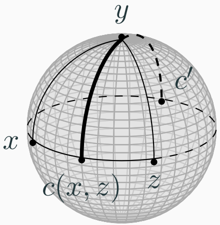

$\mathcal{M} = \mathbb{S}^2$

Intrinsic model of infimal convolution

- For $F, G\colon \mathbb{R}^n \to \mathbb{R}$ one-homogeneous:

$$\inf_{u=v+w} F(v) + G(w) = \tfrac{1}{2}\inf_{u=\frac{1}{2}(v+w)} F(v) + G(w)$$

$\Rightarrow$ Set $u = \gamma_{\widehat{v,w}}(\tfrac{1}{2})$ and obtain

$$\mathcal{E}_{\mathrm{IC}}^{\mathrm{int}}(v,w) = \frac{1}{2}\sum_{p\in\mathcal{G}} \mathrm{d}^2_{\mathcal{M}}(\gamma_{\widehat{v_p,w_p}}(\tfrac{1}{2}), f_p) + \alpha\,(\beta\,\mathrm{TV}(v) + (1-\beta)\,\mathrm{TV}_2(w))$$

- relax to d_2^2, TV_ε, $\mathrm{TV}_{2,\varepsilon}$
- compute gradients [Bačák et al., 2016]
- perform gradient descent [Absil, Mahony, Sepulchre, 2008]
- both $v, w\colon \mathcal{G} \to \mathcal{M}$ are given on the manifold

Intrinsic model of infimal convolution

- For $F, G\colon \mathbb{R}^n \to \mathbb{R}$ one-homogeneous:

$$\inf_{u=v+w} F(v) + G(w) = \tfrac{1}{2} \inf_{u=\frac{1}{2}(v+w)} F(v) + G(w)$$

$\Rightarrow$ Set $u = \gamma_{\widehat{v,w}}(\frac{1}{2})$ and obtain

$$\mathcal{E}_{\mathrm{IC}}^{\mathrm{int}}(v,w) = \frac{1}{2}\sum_{p\in\mathcal{G}} \mathrm{d}_2^2(v_p, f_p, w_p) + \alpha\,(\beta\,\mathrm{TV}(v) + (1-\beta)\,\mathrm{TV}_2(w))$$

- relax to d_2^2, TV_ε, $\mathrm{TV}_{2,\varepsilon}$
- compute gradients [Bačák et al., 2016]
- perform gradient descent [Absil, Mahony, Sepulchre, 2008]
- both $v, w\colon \mathcal{G} \to \mathcal{M}$ are given on the manifold

Example: spherical signal & intrinsic model

Let $f\colon \{1,\ldots,192\} \to \mathbb{S}^2$ be a piecewise geodesic signal

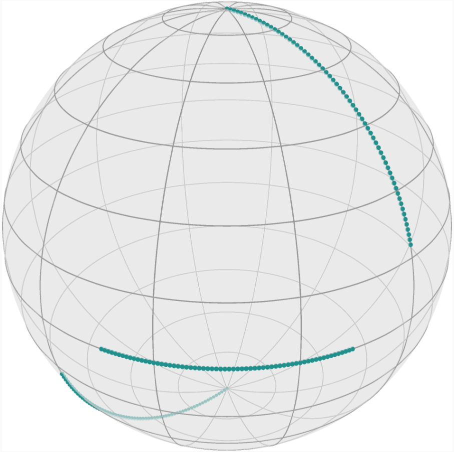

The $\mathbb{S}^2$-valued signal f

Example: spherical signal & intrinsic model

Let $f\colon \{1,\ldots,192\} \to \mathbb{S}^2$ be a piecewise geodesic signal

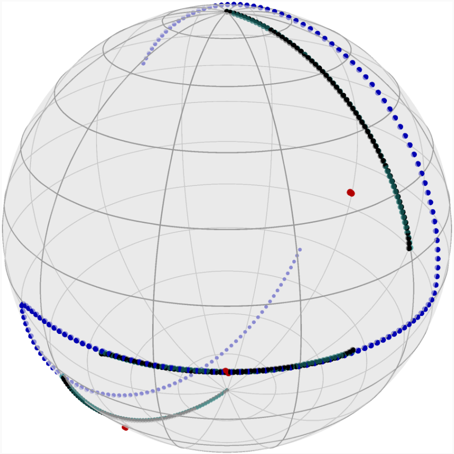

$\alpha = \frac{11}{100}$, $\beta = \frac{1}{11}$: Decompose $u \approx f$ into
v (red) piecewise constant and w (blue) piecewise geodesic

Example: ellipses & intrinsic model

symmetric positive definite matrices of size 2×2.

u_0

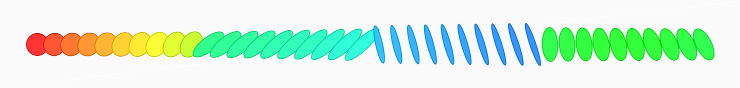

Example: ellipses & intrinsic model

symmetric positive definite matrices of size 2×2.

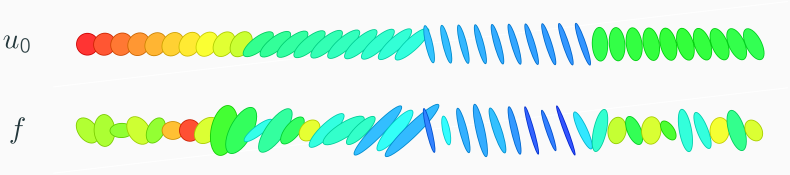

Example: ellipses & intrinsic model

symmetric positive definite matrices of size 2×2.

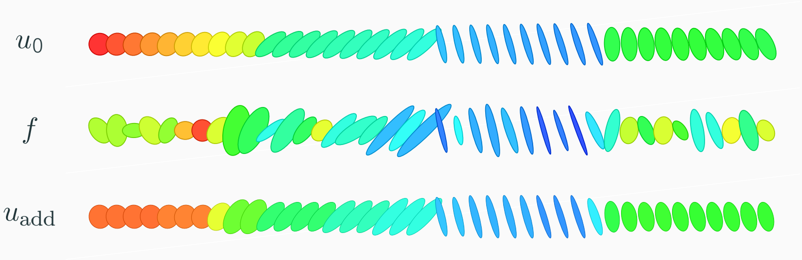

Example: ellipses & intrinsic model

symmetric positive definite matrices of size 2×2.

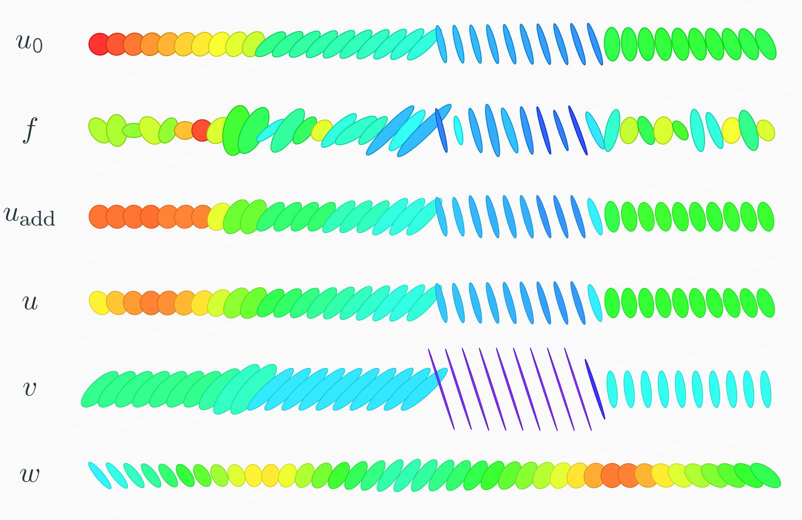

Example: EBSD, extrinsic and intrinsic model

A magnesium grain with a subgrain boundary

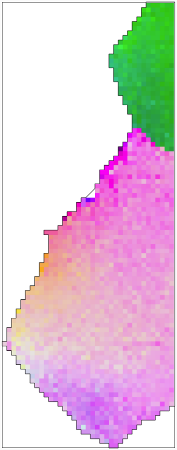

Original

data source & colorization: MTEX
[Bachmann, Hielscher, since 2005]

Example: EBSD, extrinsic and intrinsic model

A magnesium grain with a subgrain boundary

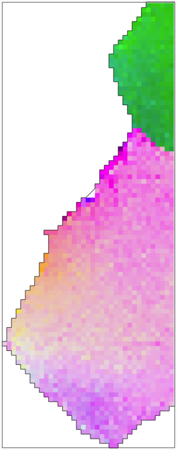

Original

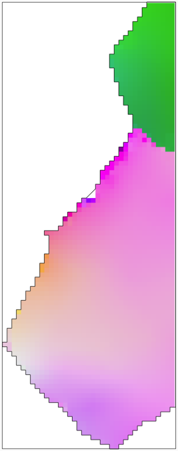

extrinsic, $\mathbb{R}^9$

$\alpha = 0.03, \beta = \frac{1}{3}$

data source & colorization: MTEX
[Bachmann, Hielscher, since 2005]

Example: EBSD, extrinsic and intrinsic model

A magnesium grain with a subgrain boundary

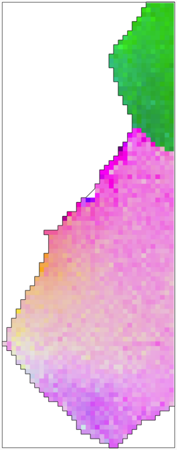

Original

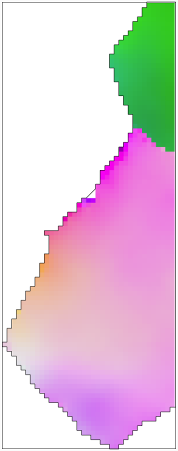

intrinsic, $\mathrm{SO}(3)$

$\alpha = 0.024, \beta = \frac{1}{4}$

data source & colorization: MTEX
[Bachmann, Hielscher, since 2005]

Example: EBSD, extrinsic and intrinsic model

A magnesium grain with a subgrain boundary

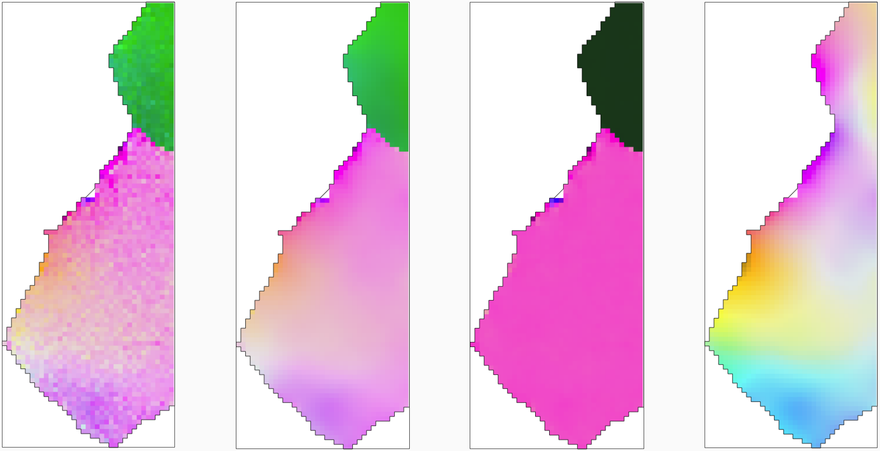

Original | intrinsic, $\mathrm{SO}(3)$ $\alpha = 0.024, \beta = \frac{1}{4}$ | v | w

data source & colorization: MTEX
[Bachmann, Hielscher, since 2005]

Summary & Conclusion

We introduced for manifold-valued images $f\colon \mathcal{G} \to \mathcal{M}$

- an extrinsic model of infimal convolution
- an intrinsic model of infimal convolution
- computed the minimizers
- implemented within the
  Manifold-valued image processing toolbox
  www.mathematik.uni-kl.de/imagepro/members/bergmann/mvirt/

Future work

- further model on Lie groups?
- other functions within the convolution?

Literature

RB, F. Laus, G. Steidl und A. Weinmann. “Second order differences of cyclic data and applications in variational denoising”. In: SIAM J. Imaging Sci. 7 (4 2014), S. 2916–2953.

A. Weinmann, L. Demaret und M. Storath. “Total variation regularization for manifold-valued data”. In: SIAM J. Imaging Sci. 7 (4 2014), S. 2226–2257.

Guy Rosman, Xue-Cheng Tai, Ron Kimmel und Alfred M Bruckstein. “Augmented-Lagrangian regularization of matrix-valued maps”. In: Methods Appl. Anal. 21.1 (2014), S. 121–138.

M. Bačák, RB, G. Steidl und A. Weinmann. “A second order non-smooth variational model for restoring manifold-valued images”. In: SIAM J. Sci. Comput. 38.1 (2016), A567–A597.

RB und A. Weinmann. “A second order TV-type approach for inpainting and denoising higher dimensional combined cyclic and vector space data”. In: J. Math. Imaging Vision 55.3 (2016), S. 401–427.